Influence of low Arctic sea-ice minima on anomalously cold Eurasian winters

Meiji Honda,[1] Jun Inoue,[2] and Shozo Yamane[3]

Received 18 December 2008; revised 8 March 2009; accepted 19 March 2009; published 28 April 2009.

[1] Influence of low Arctic sea-ice minima in early autumn on the wintertime climate over Eurasia is investigated. Observational evidence shows that significant cold anomalies over the Far East in early winter and zonally elongated cold anomalies from Europe to Far East in late winter are associated with the decrease of the Arctic sea-ice cover in the preceding summer-to-autumn seasons. Results from numerical experiments using an atmospheric general circulation model support these notions. The remote response in early winter is regarded as a stationary Rossby wave generated thermally through an anomalous turbulent heat fluxes as a result of anomalous ice-cover over the Barents-Kara Seas in late autumn, which tends to induce an amplification of the Siberian high causing colder conditions over the Far East. The late-winter cold anomalies over Eurasia are also reproduced in our experiment, which is associated with the negative phase of the North Atlantic Oscillation. **Citation:** Honda, M., J. Inoue, and S. Yamane (2009), Influence of low Arctic sea-ice minima on anomalously cold Eurasian winters, *Geophys. Res. Lett.*, *36*, L08707, doi:10.1029/2008GL037079.

1. Introduction

[2] Summertime Arctic sea-ice cover has experienced an accelerated decline during the last 10 years [e.g., *Comiso et al.*, 2008]. After the record minimums of the Arctic ice extent in September 2005 and 2007 (Figure 1a), however, strong cold waves often attacked the Central-to-East Asian countries in the following winters, which caused anomalous low temperatures and extraordinary heavy snowfall over Japan in December 2005 [e.g., *Takano et al.*, 2008], and over the southern part of China in January–February 2008 [e.g., *Tokyo Climate Center*, 2008]. Recent model studies have suggested that wintertime sea-ice variability influences the atmospheric circulation through the formation of stationary Rossby wave trains in the North Pacific sector [*Honda et al.*, 1999; *Yamamoto et al.*, 2006], and through the modification of the storm track in the North Atlantic sector [*Alexander et al.*, 2004; *Magnusdottir et al.*, 2004; *Kvamstø et al.*, 2004]. Possible influence of the winter Arctic sea-ice variability on the mid-latitude atmospheric circulation through synoptic transient eddy forcings is indicated by *Glowienka-Hense and Hense* [1992]. *Seierstad and Bader* [2008] showed that a projected future Arctic sea-ice reduction for all the seasons induce a negative phase of the North Atlantic Oscillation (NAO) in late winter. In the present study, we mainly focus on the "summertime" Arctic sea-ice influence on the "wintertime" Eurasian climate variability through statistical analyses using a reanalysis data, and numerical experiments using an atmospheric general circulation model (AGCM).

2. Observational Analysis

[3] The sea-ice concentration data used in this study, which covers the period 1978–2007, is a Met Office Hadley Centre's sea ice and sea surface temperature data set version 1 (HadISST1) [*Rayner et al.*, 2003], which is the monthly globally complete fields on a one degree latitude–longitude grid. The atmospheric data used here is a reanalysis data by the National Centers for Environmental Prediction and National Centers for Atmospheric Research jointly [*Kalnay et al.*, 1996] compiled on a 2.5 × 2.5 regular latitude-longitude grid. We use the monthly–mean data for the 28 summer-to-winter seasons (1978/79–2005/2006).

[4] Considering that the sea ice has substantially declined along the Siberian coast (SC) [e.g., *Ogi and Wallace*, 2007; *Inoue and Kikuchi*, 2007], we defined the Siberian coast ice extent index (SCI) as the area mean ice concentration within the areas of 72°–82°N, 30°E–180° from the Barents to East Siberian Seas (Figure 1a). The SCI time series of September (SCI–SEP) is shown in Figure 1b. In the analyses, we have removed the linear trend prior to computing regressions and correlations. To examine a relationship between the summer Arctic sea ice and the following winter Eurasian weather conditions, monthly-mean 1000-hPa air temperature (T_{1000}) anomalies for December and February are regressed linearly on the preceding SCI–SEP, respectively (Figure 2). It is noted that the signs are reversed to emphasize the decrease of air temperatures associated with the sea-ice reduction. As shown in Figure 2a, significant cold anomalies are centered on the Far East (eastern part of Eurasia) in December, which are associated with an intensified Siberian high in the sea-level pressure (SLP) field (not shown). In February, significant cold anomalies are zonally elongated from Europe to the East Asia (Figure 2b), associated with negative NAO-like anomalies in SLP field (not shown). These characteristics are qualitatively comparable with the climate anomalies of December 2005 and January–February 2008, respectively.

3. Experimental Design

[5] In order to quantitatively examine influences of the summertime Arctic sea-ice anomalies on the atmospheric

[1]Research Institute for Global Change, Japan Agency for Marine-Earth Science and Technology, Yokohama, Japan.
[2]Research Institute for Global Change, Japan Agency for Marine-Earth Science and Technology, Yokosuka, Japan.
[3]Department of Environmental Systems Science, Doshisha University, Kyotanabe, Japan.

0094-8276/09/2008GL037079

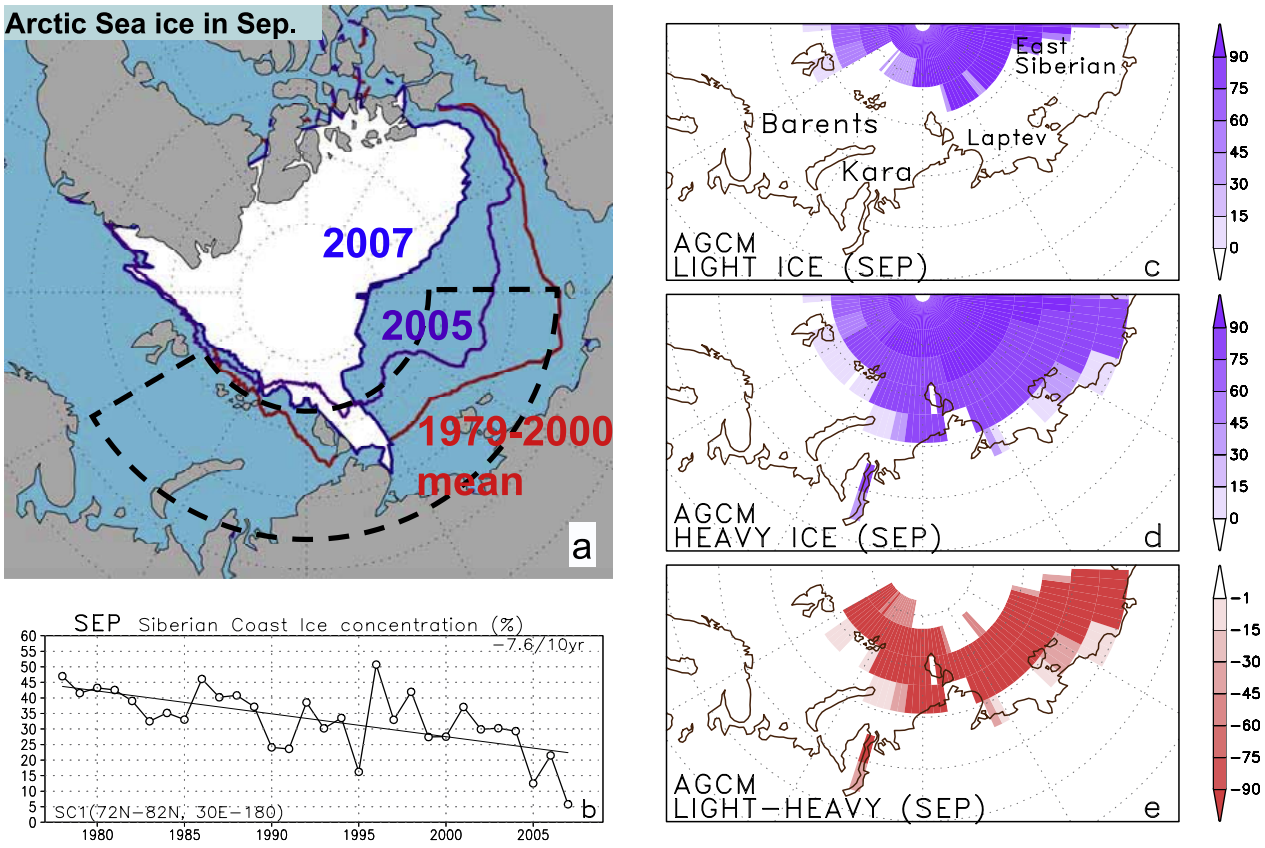

Figure 1. (a) Arctic sea-ice distribution in September. Solid lines indicate 50% sea-ice concentration for 2007 (blue), 2005 (purple), and mean for 1979-2000 (red). (b) September time series of mean sea-ice concentration (open circle; %) and its linear trend (solid straight line) for 1978–2007 averaged over the Siberian coast (SC), defined as the areas of 72°–82°N, 30°E–180° (region indicated by dashed lines in panel a). (c–d) Sea ice setting as the model boundary condition for the (c) light and (d) heavy ice cases on September 1st. Values denote sea-ice concentration (%). (e) Difference of ice concentration between them (light minus heavy).

circulation, we execute an ideal experiment using an AGCM. In the present study, we use the AFES (AGCM for the Earth Simulator) developed at Japan Agency for Marine-Earth Science and Technology, which is a global primitive equation model with a spectral transform method [*Ohfuchi et al.*, 2004]. We use a particular version of the model with a triangular truncation at horizontal wavenumber 42 (approximately 2.8° horizontal resolution) and 20 vertical levels (top: 8 hPa). In the model, sea-ice cover and sea surface temperature (SST) are prescribed as boundary conditions, respectively.

[6] A sensitivity experiment of the atmospheric response to the summer-to-autumn Arctic sea-ice variability was performed as follows. Based on the climatological mean sea-ice concentration for the period 1979–2000 in the SC region (Figure 1a), two sets of sea-ice boundary conditions (heavy and light) in the model from September to December. In the heavy ice case, we set the prescribed IC as 90% where the climatological IC is between 15% and 90%. In the light ice case, on the other hand, the prescribed IC is set as 0% where the climatological IC is less than 90%. The climatological-mean SST is prescribed where ice is absent. Figures 1c–1e show the model ice-boundary conditions and their difference on September 1st. First we performed a control run for 55 years under the climatological sea-ice and SST conditions. A pair of the 6–month model integrations from September to February with the heavy and light ice cases was repeated 50 times with different initial atmospheric and land-surface conditions on September 1st taken from the 6th to 55th model year. It is noted that there are no differences in the ice-boundary conditions in January and February. In order to emphasize signals of sea-ice anomalies, we focus on the monthly-mean difference field (the light minus heavy ice cases) averaged over the 28 integrations (years 6–16 and 27–43). If we use all the 50 integrations, tendencies of results are similar, but signals are generally weak. Actually, we see a decadal-like modulation in the control run, which may be associated with land-surface processes. It is also confirmed that there are significant differences between the averaged initial conditions for the selected 28 years and other 22 years. This issue relating to the preconditioning of atmospheric responses needs to be investigated in future studies.

4. Results

[7] Model-simulated differences of the surface air temperature (SAT) between the light and heavy ice cases are

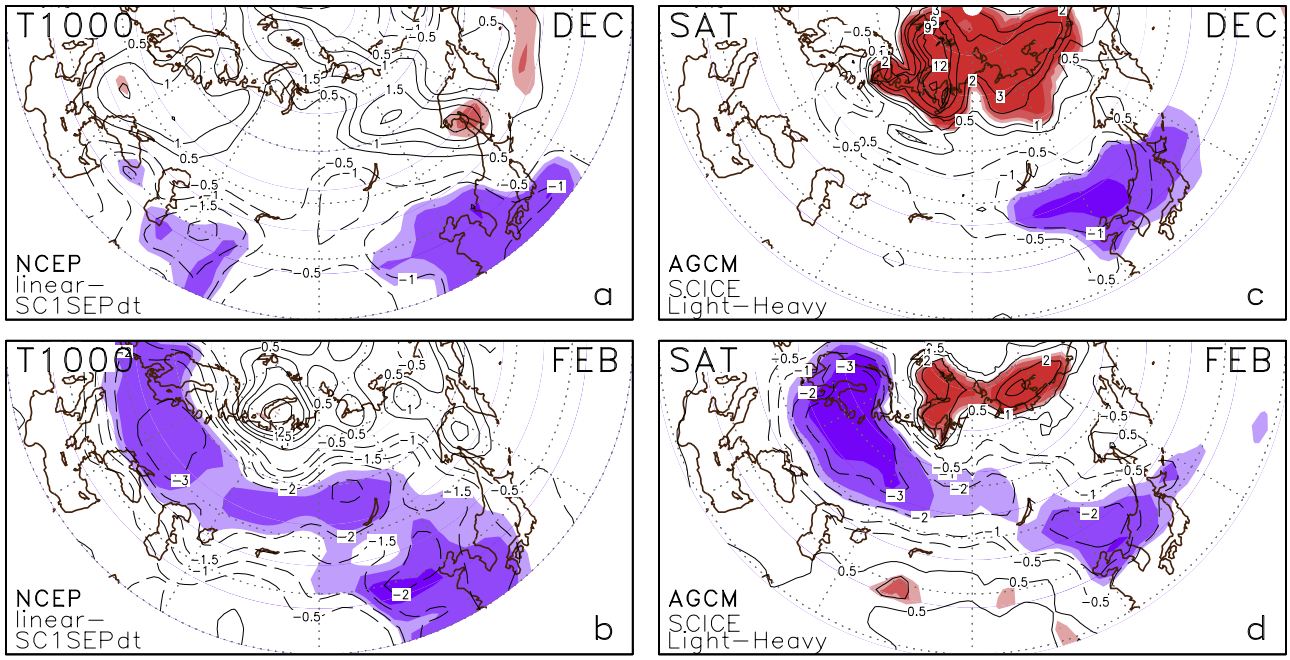

Figure 2. Maps of monthly-mean 1000-hPa air temperature (T_{1000}) for (a) December and (b) February for 1978/79–2005/06 regressed linearly on the ice-concentration over SC (SCI) in previous September for 1978–2005. The signs are reversed to emphasize the reduced-ice condition. Contours correspond to T_{1000} local changes (degrees) when the SCI "decreases" by the two standard deviations. Areas of light, moderate, and heavy color shading indicate that the correlation between the T_{1000} and SCI is significant at the 90%, 95%, and 99% confidence levels, respectively, based on Student's *t* test. AGCM-simulated differences in surface air temperature (degrees; SAT) for (c) December, and (d) February between the ensemble means simulated with the light and heavy ice cases (light minus heavy). Light, moderate, and heavy color shadings indicate the differences significant at the 90% 95% 99% confidence levels, respectively. Outer circle is 30°N.

characterized by significant cold anomalies centered over the Far East in December (Figure 2c) and those for zonally elongated signature from Europe to the Far East (Figure 2d), which are highly consistent with the observational results (Figure 2).

[8] We determine that the cooler conditions over the Far East observed in December (Figures 2a and 2c) are triggered by a stationary Rossby wave emanating from the anomalous ice cover in the Barents–Kara Seas (BK) in late autumn. Figures 3a–3c show the model-simulated differences in November. The 250-hPa geopotential height (Z_{250}) response (Figure 3a) displays a significant wavelike anomalies across Eurasia, which are associated with the propagation of wave-activity flux as indicated by the arrows [*Takaya and Nakamura*, 2001]. It is estimated from the Z_{250} difference field and suggests that this wavetrain is associated with a stationary Rossby wave excited around BK.

[9] The corresponding SLP difference map shown in Figure 3c is characterized by cyclonic anomalies over the northern part of Barents Sea and anticyclonic anomalies extending from the East European to the West Siberian Plains. Interestingly, the upper tropospheric pattern (Figure 3a) shifts upstreamward by about a quarter wave length relative to the SLP pattern, which reflects the barolinic nature of the response. Figure 4a shows a vertical cross section of the model simulated difference in geopotential height along the tropospheric wave train shown in Figure 3a. Superimposed arrows in the difference field in Figure 4a are the vertical and horizontal components of the wave activity flux. The lower tropospheric response is baroclinic and thus favors upward emanation of wave activity, and the horizontal component is dominantly downstreamward in the upper troposhere, which indicates that the stationary Rossby wave emanates from the lower levels around BK. The force behind the flux is likely the anomalous low-level diabatic heating through the sensible and latent heat fluxes over BK (Figure 4b), caused by the distribution-difference of the local sea-ice cover. We identify these heat flux anomalies as primary heating and cooling sources for this response. Evidently, the upward component of the wave activity flux is apparent just over the pair of the heating and cooling sources. The above diagnosis is consistent with the result of *Honda et al.* [1999], which shows that a stationary Rossby wave train is forced by the anomalous heat flux associated with sea-ice cover in the Sea of Okhotsk. It is noted that the anomalous diabatic heating over BK is rather small in September, and becomes apparent in October and November over BK in our experiment, which is consistent with the result of *Seierstad and Bader* [2008].

[10] We next discuss how the stationary Rossby wave emanating in November causes cold anomalies over the Far East in December. A weakening of storm-track activity along 60°N between the anticylonic anomalies to the north and cyclonic anomalies to the south in the upper troposphere (Figure 3b) means that anomalous feedback forcing

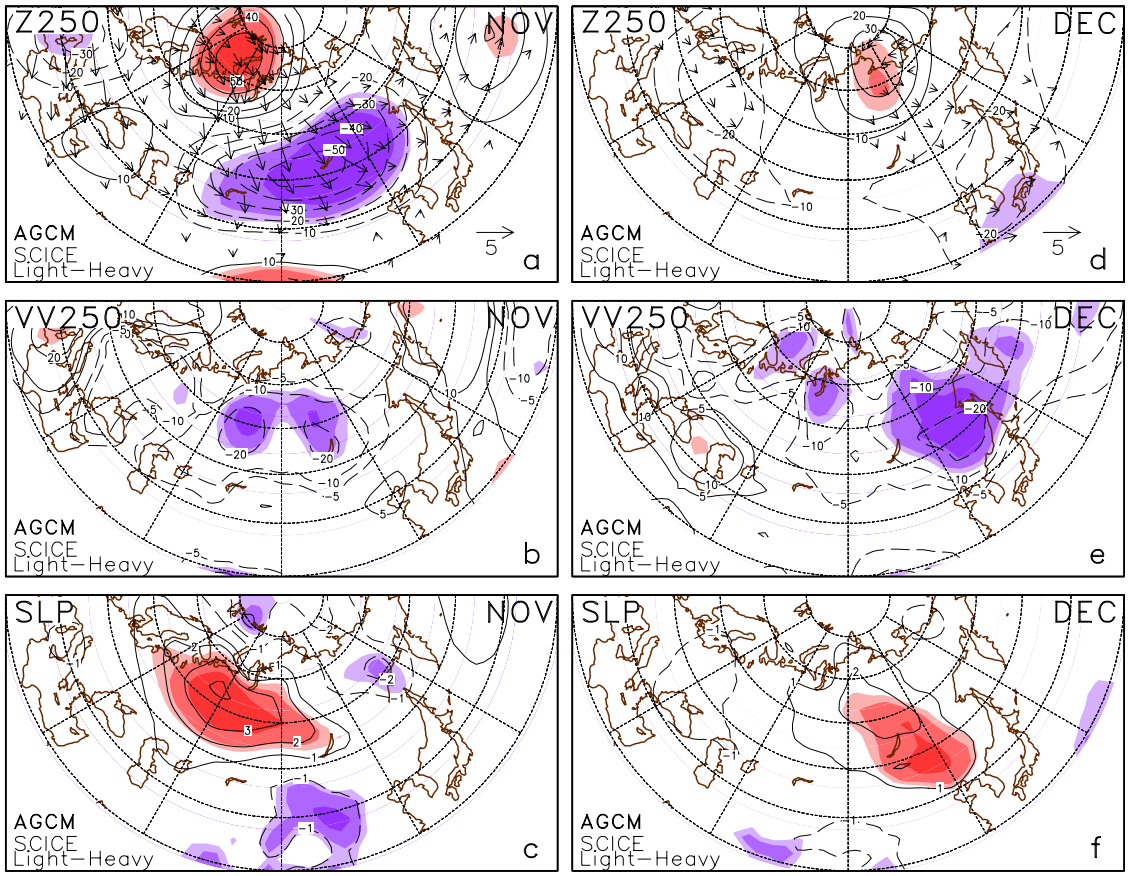

Figure 3. Same as in Figures 2c and 2d but for (a) 250-hPa geopotential height anomalies (m; Z_{250}), (b) variance of 250-hPa meridional velocity associated with transient eddies with periods shorter than five days ($m^2\ s^{-2}$), and (c) sea-level pressure (hPa; SLP) in November. Superimposed arrows in Figure 3a indicate the horizontal component of a wave-activity flux ($m^2\ s^{-2}$) at that level formulated by *Takaya and Nakamura* [2001]. Heavy solid line in Figure 3a denotes vertical cross section in Figure 4a. (d–f) Same as in (Figures 3a–3c) but for December.

from high frequency transient eddies is likely to contribute toward the amplification and maintenance of the incipient meridional dipole structures through meridional anomalous vorticity flux [e.g., *Lau and Nath*, 1991]. In December, the region for the weak storm-track activity reaches over the northeastern Siberia (Figure 3e), maintaining the upper tropospheric meridional dipole structure (Figure 3d), although the mechanism of eastward propagation is still unclear. Since the climatological core of a low-level cold air mass is located in the northeastern Siberia, the anomalous easterly wind induced at the surface by the upper-level anticyclonic anomalies yields anomalous cold advection southwestward. The anomalous cold air piling up over near the Lake Bikal contributes to the amplification of the Siberian high (Figure 3f) [*Takaya and Nakamura*, 2005]. Consequently, cold northerlies by the development of the surface high through the above process brings cold air mass extensively over the Far East (Figure 2c).

[11] The zonally elongated cold anomalies over Eurasia observed and simulated in February (Figures 2b and 2d) are associated with negative phase of the NAO (not shown). Wintertime negative feedback between the NAO and sea-ice variability over the Atlantic sector [e.g., *Alexander et al.*, 2004] supports that less sea-ice condition in the Barents Sea tends to cause the weakening of the Icelandic low in late winter [e.g., *Yamamoto et al.*, 2006; *Seierstad and Bader*, 2008]. Although there are no differences in the ice boundary conditions in January and February in our experiment, there is a hint of the late winter response in the significant warm anomalies over the Arctic Ocean (Figures 2c–2d), which may be related to snow-amount anomalies over there (not shown). It is noted that substantially warmer conditions over the Arctic Ocean were observed through the winter 2005/06 and 2007/08 (not shown). Further, heavy snow-cover anomalies along southern edge over Eurasia are identified through winter in the light-ice cases (not shown). Long-lasting anomalous snow-cover may be one of possible communicators for this late winter response to summer-to-autumn Arctic sea-ice anomalies. These findings are consistent with *Deser et al.* [2007], which suggests that an equilibrium NAO-like response forced by sea-ice anomaly induced diabatic heating is reached in 2–3 months. Further investigation should be required for understanding the delayed response.

5. Summary

[12] A relationship between the minimum Arctic sea-ice extent anomalies on wintertime Eurasian climate was iden-

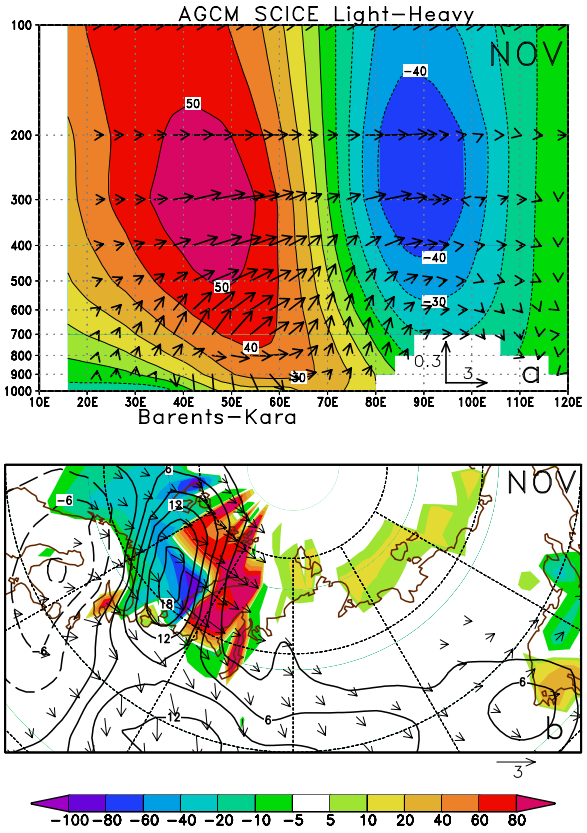

Figure 4. (a) Vertical-horizontal cross section of AGCM-simulated differences in geopotential height anomalies (m) in November along the heavy solid line in Figure 3a. Superimposed arrows indicate the vertical-horizontal component of a wave-activity flux (m^2 s^{-2}). (b) AGCM-simulated differences in total of surface sensible and latent heat fluxes (Wm^{-2}; positive: upward) for November (shaded). The 500–250-hPa averaged horizontal and 700-hPa vertical components of a wave-activity flux (m^2 s^{-2}) are shown by arrows and contours, respectively. Outer circle is 60°N.

tified in an analysis based on observational studies, and examined through a sensitivity experiment using an AGCM. The summer Arctic sea-ice reduction along the Siberian coast tends to reduce ice cover of the Barents–Kara Seas in late autumn. Near-surface anomalous diabatic heating associated with the anomalous sea-ice cover becomes apparent in late autumn, which tends to excite a stationary Rossby wave train in November. The wave train propagates southeastward, and forms anticyclonic anomalies over the Barents Sea and cyclonic anomalies over central Eurasia in the upper troposphere in the light ice case. The upper tropospheric height anomalies thus-formed are maintained through feedback forcing from high frequency transient eddies. Eastward propagation of the height anomalies toward the Far East in December tends to induce near surface amplification of the Siberian high in the light ice case, which intensifies cold northerlies over the Far East. The zonally elongated cold anomalies over Eurasia in late winter are also reproduced in our experiment. This cold temperature anomalies are associated with the negative phase of the NAO, which is consistent with several former studies, although we have to consider what are mechanisms for the delayed response.

[13] Does the recent rapid decrease in the summertime Arctic sea-ice extent enhance the wintertime cold anomalies over Eurasia? Perhaps, but perhaps not, since other surface conditions in addition to sea ice display anomalies (e.g., SST, snow, and land parameters) that can impact the atmospheric circulation. Further, since the basic state of the atmospheric circulation is gradually changing, atmospheric responses to a future decrease of the sea-ice may differ from that for the present one.

[14] **Acknowledgments.** We thank H. Nakamura and K. Takaya for valuable comments and stimulating discussion. The Grid Analysis and Display System (GrADS) was used for drawing figures. This work was supported in part by the Japan Society for the Promotion of Science, Grant-in-Aid for Scientific Research (A) 18204044, and Grant-in-Aid for Scientific Research (C) 18540441.

References

Alexander, M. A., U. S. Bhatt, J. E. Walsh, M. S. Timlin, J. S. Miller, and J. D. Scott (2004), The atmospheric response to realistic Arctic sea ice anomalies in an AGCM during winter, *J. Clim.*, *17*, 890–905.

Comiso, J. C., C. L. Parkinson, R. Gersten, and L. Stock (2008), Accelerated decline in the Arctic sea ice cover, *Geophys. Res. Lett.*, *35*, L01703, doi:10.1029/2007GL031972.

Deser, C., R. A. Tomas, and S. Peng (2007), The transient atmospheric circulation response to North Atlantic SST and sea ice anomalies, *J. Clim.*, *20*, 4751–4767.

Glowienka-Hense, R., and A. Hense (1992), The effect of an arctic polynya on the Northern Hemisphere mean circulation and eddy regime: A numerical experiment, *Clim. Dyn.*, *7*, 155–163.

Honda, M., K. Yamazaki, H. Nakamura, and K. Takeuchi (1999), Dynamic and thermodynamic characteristics of atmospheric response to anomalous sea-ice extent in the Sea of Okhotsk, *J. Clim.*, *12*, 3347–3358.

Inoue, J., and T. Kikuchi (2007), Outflow of summertime Arctic sea ice observed by ice drifting buoys and its linkage with ice reduction and atmospheric circulation patterns, *J. Meteorol. Soc. Jpn.*, *85*, 881–887.

Kalnay, E., et al. (1996), The NCEP/NCAR 40-year reanalysis project, *Bull. Am. Meteorol. Soc.*, *77*, 437–471.

Kvamstø, N. G., P. Skeie, and D. B. Stephenson (2004), Impact of Labrador sea-ice extent on the North Atlantic Oscillation, *Int. J. Climatol.*, *24*, 603–612.

Lau, N.-C., and M. J. Nath (1991), Variability of the baroclinic and barotropic transient eddy forcing associated with monthly changes in the midlatitude storm tracks, *J. Atmos. Sci.*, *48*, 2589–2613.

Magnusdottir, G., C. Deser, and R. Saravanan (2004), The effects of North Atlantic SST and sea ice anomalies on the winter circulation in CCM3. Part I: Main features and storm track characteristics of the response, *J. Clim.*, *17*, 857–876.

Ogi, M., and J. M. Wallace (2007), Summer minimum Arctic sea ice extent and the associated summer atmospheric circulation, *Geophys. Res. Lett.*, *34*, L12705, doi:10.1029/2007GL029897.

Ohfuchi, W., H. Nakamura, M. K. Yoshioka, T. Enomoto, K. Takaya, X. Peng, S. Yamane, T. Nishimura, Y. Kurihara, and K. Ninomiya (2004), 10-km mesh meso-scale resolving simulations of the global atmosphere on the Earth Simulator—Preliminary outcomes of AFES (AGCM for the Earth Simulator), *J. Earth Simulator*, *1*, 8–34.

Rayner, N. A., D. E. Parker, E. B. Horton, C. K. Folland, L. V. Alexander, D. P. Rowell, E. C. Kent, and A. Kaplan (2003), Global analyses of sea surface temperature, sea ice, and night marine air temperature since the late nineteenth century, *J. Geophys. Res.*, *108*(D14), 4407, doi:10.1029/2002JD002670.

Seierstad, I. A., and J. Bader (2008), Impact of a projected future Arctic sea ice reduction on extratropical storminess and the NAO (online), *Clim. Dyn.*, doi:10.1007/s00382-008-0463-x.

Takano, Y., Y. Tachibana, and K. Iwamoto (2008), Influence of large-scale atmospheric circulation and local sea surface temperature on convective activity over the Sea of Japan in December, *Sci. Online Lett. Atmos.*, *4*, 113–116.

Takaya, K., and H. Nakamura (2001), A formulation of a phase-independent wave-activity flux for stationary and migratory quasigeostrophic eddies on a zonally varying basic flow, *J. Atmos. Sci.*, *58*, 608–627.

Takaya, K., and H. Nakamura (2005), Mechanisms of intraseasonal amplification of the cold Siberian high, *J. Atmos. Sci.*, *62*, 4423–4440.

Tokyo Climate Center (2008), Summary of Asian winter monsoon 2007/2008—Extremely low temperatures in Asia, *TCC News*, *12*, pp. 5–7.

Yamamoto, K., Y. Tachibana, M. Honda, and J. Ukita (2006), Intra-seasonal relationship between the Northern Hemisphere sea ice variability and the North Atlantic Oscillation, *Geophys. Res. Lett.*, *33*, L14711, doi:10.1029/2006GL026286.

M. Honda, Research Institute for Global Change, Japan Agency for Marine-Earth Science and Technology, Yokohama 236-0001, Japan. (meiji@jamstec.go.jp)

J. Inoue, Research Institute for Global Change, Japan Agency for Marine-Earth Science and Technology, Yokosuka 237-0061, Japan. (jun.inoue@jamstec.go.jp)

S. Yamane, Department of Environmental Systems Science, Doshisha University, Kyotanabe 610-0394, Japan. (syamane@mail.doshisha.ac.jp)